Complex Dynamics of Nonlinear Oscillations of Hair Bundles of Auditory Hair Cell Regulated by Memristor

Ben CAO [1,*]，Kai-Hua MA [2]

1. School of Artificial Intelligence, Nanjing University of Information Science and Technology, Nanjing, Jiangsu, China, 210044

2. School of Mathematics and Physics, Jiangsu University of Technology, Changzhou, Jiangsu, China, 213001

Abstract: The nonlinear oscillations of hair bundles of auditory hair cell are important for sound perception. Memristors, as electronic components highly similar to the behavior of neurons and synapses, show potential in neuromodulation. The present paper, for the first time, introduces memristors into the regulation of hair bundle mechanical vibrations, constructs a dynamical model with memristor coupling, and investigates the regulatory dynamics of coupling strength (γ) on oscillation modes through simulation and bifurcation analysis. The results show that as γ increases, the hair bundle oscillation patterns exhibit a variety of complex patterns, including different types of spiking, bursting, and chaos. Bifurcation analysis and Lyapunov exponents validate the dynamic process of mode transitions, indicating that memristors influence oscillation patterns by regulating the adaptation force of hair bundle. Moreover, bifurcation analysis in the two-parameter plane indicates that increasing γ can expand the oscillation region of the hair bundle, but excessive coupling can suppress oscillations. Under specific parameter combinations, the system exhibits insensitivity to memristor regulation, reflecting the robustness of the auditory system. This study provides a theoretical basis for understanding the nonlinear characteristics of auditory function and developing novel neuromodulation technologies.

Keywords: Nonlinear oscillation; Bifurcation; Hair cell; Memristor; Neuromodulation

1 Introduction

The auditory system achieves sound perception in complex environments through unique physiological structures, such as detecting faint sounds in quiet or perceiving specific sounds in noise[1]. The realization of these important auditory functions relies on the nonlinear oscillations of hair bundles of hair cell[2,3]. The mechanical oscillations of sound signals, once captured by the hair bundles, influence the opening and closing of the mechanoelectrical transduction (MET) ion channels in the hair bundles[4]. This process converts mechanical signals into electrical signals, which are then transmitted to the brain via the auditory nerve to form auditory perception. Numerous experimental studies have demonstrated that hair bundles exhibit a variety of complex dynamical behaviors related to auditory functions. For example, multimodal spontaneous oscillations associated with sound amplification functions[5–7], and “twitch” forced oscillations of hair bundles in quiescent state related to adaption functions[8,9]. In particular, recent studies have found that the efferent system can regulate the dynamics of hair cell bundles through the efferent auditory nerve, thereby modulating their sensitivity to external mechanical stimuli[10,11]. These complex nonlinear experimental phenomena can be well explained through dynamical analysis methods such as bifurcation, chaos, and vector fields, which provide the possibility for us to understand and utilize auditory functions[12–14]. More importantly, it has inspired the idea that auditory sensitivity can be regulated through neuromodulation, which can be used to enhance auditory function, treat hearing disorders, and improve the

design of cochlear implants.

Neuromodulation is one of the most promising approaches for treating neurological and brain disorders, encompassing a variety of methods such as optogenetics, electrical stimulation, magnetic stimulation, and ultrasound[15]. Memristors are an important tool for implementing neuromodulation[16]. The memristor is the fourth fundamental circuit element that describes the relationship between charge and magnetic flux, first proposed by Chua[17]. In recent years, due to its high similarity to biological neurons and synapses, the memristor has often been used to simulate synapses[18,19]. The memristor couples with neurons through electromagnetic induction effects and regulates their electrical activity by influencing the membrane potential of neurons via applied electromagnetic induction currents[20,21]. Although the memristor has been extensively studied in simulating neuronal electrical activity[22–25], its application in neuromodulation, regulation of nervous system functions, or treatment of diseases remains to be further explored. This is especially true for the auditory system, which involves the coupling of neuronal electrical activity and the mechanical motion of hair cells[26–28], making the problem more challenging.

In the present paper, for the first time, applies memristors to regulate the mechanical oscillations of auditory hair cell bundles. By utilizing the electromagnetic induction effect of memristors, the adaptation force for the opening and closing of the MET channels in hair cells is regulated, which in turn modulates the mechanical oscillations of the hair bundles, with the expectation of regulating auditory function. A dynamical model of hair bundle regulation by memristors has been constructed to investigate the impact of different coupling strengths on mechanical oscillation patterns. Bifurcation analysis was employed to obtain the transition dynamics of oscillation pattern, laying the foundation for utilizing memristors to regulate auditory function and treat auditory disorders.

2 Model and method

The schematic diagram of the mechanical oscillations of hair bundles of hair cell regulated by the memristor is shown in Fig. 1. The theoretical model is constructed as follows:

$$\begin{cases} \lambda \dfrac{\mathrm{d}X}{\mathrm{d}t} = -K_{GS}(X - X_a - DP_0) - K_{SP}X + F & (1.1) \\ \lambda_a \dfrac{\mathrm{d}X_a}{\mathrm{d}t} = K_{GS}(X - X_a - DP_0) - K_{ES}(X_a - X_{ES}) - F_a & (1.2) \\ \dfrac{\mathrm{d}\phi}{\mathrm{d}t} = k_1 X - k_2 \phi & (1.3) \end{cases} \tag{1}$$

Equations (1.1) and (1.2) represent the classical model of hair bundle mechanical oscillations[9]. where X and X_a is the displacement of the hair bundle and the myosin motor, respectively. P_0 is the opening probability of MET channel shown as follow:

$$P_o = 1/(1 + A\exp(\frac{-K_{GS}D(X - X_a)}{Nk_bT})) \tag{2}$$

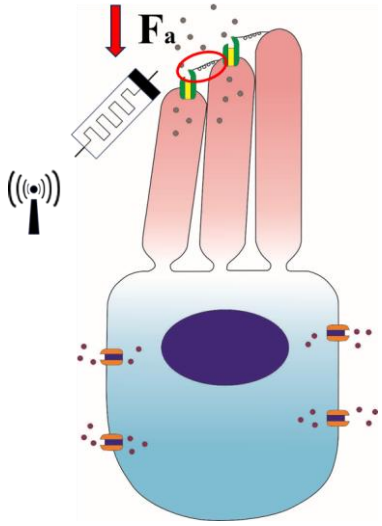

Fig. 1 The schematic diagram of the mechanical movement of hair bundles of hair cell regulated by memristor

A is related to the open probability of MET channel when the gating spring is severed, shown as follow:

$$A = \exp([10k_bT + (K_{GS}D^2)/(2N)]/(k_bT)) \tag{3}$$

F_a is the force associated with biological adaptation. Without the regulation of memristor, F_a is shown as follow:

$$F_a = F_{\max}(1 - SP_0) \tag{4}$$

Equation (1.3) represents the magnetic flux across the MET channel. The flux has a time-varying characteristic and affects the ion concentration entering and exiting the MET channel through electromagnetic induction, thereby influencing F_a. After regulation by the memristor, the expression for F_a becomes:

$$F_a = F_{\max}(1 - SP_0) + \gamma W(\phi) \tag{5}$$

Where γ is the coupling strength of memristor regulation on the mechanical behavior of hair bundles, $W(\varphi)$ is the magnetic flux-controlled memristor, consistent with previous studies[21,29,30].

$$W(\phi) = \alpha + 3\beta\phi^2 \tag{6}$$

D is the "gating swing" which affects the function of P_0 to affect the strength of calcium ion regulation and S is the strength of calcium ion feedback, which is closely related to extracellular calcium ion concentration. These two parameters are related to the regulation of mechanical movement and are the key parameters in the present paper. The values and meanings of the remaining parameters are shown in Table 1.

The model equations are numerically integrated using the fourth-order Runge-Kutta method, with a time step of 0.01 ms. Bifurcation analysis is generated using the software XPPAUTO[31].

Table 1 The values and meanings of parameters for the model

Parameters	Magnitude	Meaning
λ	0.28 μNs/m	The damping coefficient of hair bundles
λ_a	10 μNs/m	The damping coefficient of myosin motor
K_{GS}	0.75 mN/m	The stiffness of gating spring
K_{SP}	1 mN/m	The stiffness of hair bundle
K_{ES}	0.25 mN/m	The constrained stiffness of gating spring
X_{ES}	0 nm	The initial position of the myosin motor
F_{max}	90 pN	The maximum of adaptation force
F	0	External force
N	50	Number of MET channels
T	295.15 K	Temperature
k_b	1.380649×10^{-23} J/K	Boltzmann constant
k_1	0.1 V/m	Parameter of memristor
k_2	0.02 s^{-1}	Parameter of memristor
α	0.02 S	Parameter of magnetic flux-controlled memristor
β	0.1 S/Wb^2	Parameter of magnetic flux-controlled memristor

3 Results

3.1 Complex oscillations of hair bundles induced by memristor

When $\gamma = 0$, the expression for the adaptation force F_a of the hair bundle degrades from Equation (5) to Equation (4). In this case, without memristor regulation, the trajectory of the hair bundle oscillations in the (X_a, X) phase plane is a definite circle which indicates the system's behavior is periodic limit cycle spiking oscillations, as shown in Fig. 2a. When $\gamma > 0$, the mechanical oscillations of the hair bundles are regulated by the memristor. When γ is small ($\gamma = 0.005$ pN/S), the memristor has a limited impact on the oscillations, only altering the position and shape of the oscillation trajectory in the phase space, while the system's behavior remains as limit cycle oscillations, as shown in Fig. 2b.

As γ is further increased ($\gamma = 0.0082$ pN/S), the regulation by the memristor causes the oscillation trajectory to transition from a definite period cycle to infinite period cycles. This implies that the memristor induces chaotic oscillations, which may be related to complex auditory functions, as shown in Fig. 2c. When $\gamma = 0.00945$ pN/S, the trajectory becomes finite period cycle again. The trajectory manifests as two large circles and two small circles, indicating that the oscillation pattern transitions to period-4 bursting oscillations, as shown in Fig. 2d. When $\gamma = 0.01063$ pN/S, the oscillations manifest as another form of chaos, with higher regularity compared to Fig. 2c, implying that this is a weaker form of chaos, as shown in Fig. 2e. When $\gamma = 0.0112$ pN/S, the trajectory of the oscillation manifest as a large circle and a finite number of many small circles, indicating that the oscillations are characterized by bursting with numerous small spikes, as shown in Fig. 2f. As γ is further increased ($\gamma = 0.0114$ pN/S), the large circle disappears, and the trajectory becomes a small circle in the upper right corner of the phase plane, at which point the system exhibits small-amplitude periodic spiking, as shown in Fig. 2g. Ultimately, when $\gamma = 0.0116$ pN/S

the trajectory vanishes, manifesting as a single point in the phase plane, indicating that the oscillations of the hair bundle are suppressed by the memristor, and the system exhibits a quiescent state, as shown in Fig. 2h.

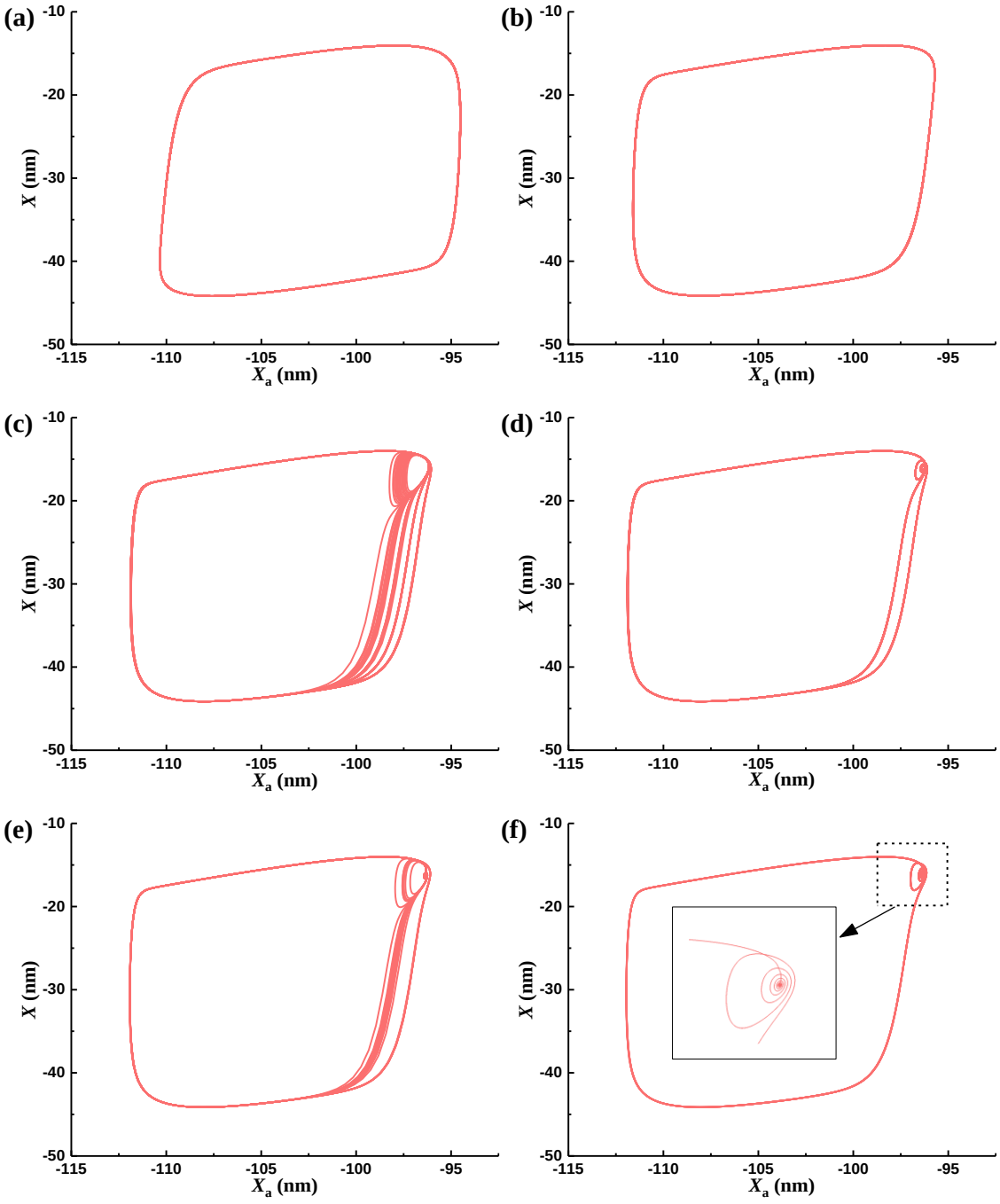

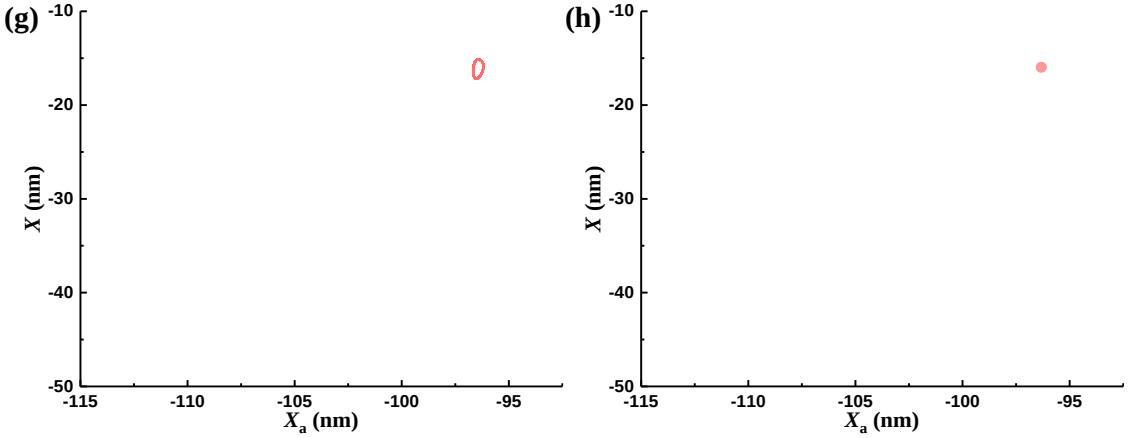

Fig. 2 The schematic diagram of the mechanical movement of hair cell bundles regulated by memristors for S = 0.95 and D = 70 nm. Trajectories of ciliary bundle motion regulated by memristors in the (X, X_a) phase space for different γ. (a) γ = 0; (b) γ = 0.005 pN/S; (c) γ = 0.0082 pN/S; (d) γ = 0.00945 pN/S; (e) γ = 0.01063 pN/S; (f) γ = 0.0112 pN/S; (g) γ = 0.114 pN/S; (h) γ = 0.0116 pN/S

3.2 The dynamical underlying the transitions of oscillation patterns regulated by memristor

Furthermore, the dynamics of transitions in hair bundle oscillation patterns regulated by memristor are investigated through bifurcation and chaos analysis, as shown in Fig. 3. When γ is small, the system exhibits the coexistence of unstable equilibrium points (black dot curve) and the stable limit cycle (green solid curve), which corresponds to periodic spiking oscillations (corresponding to Figs. 2a and b), as shown in Fig. 3a. As γ increases, the stable limit cycle becomes unstable (blue dot curve) through a fold (saddle-node) bifurcation of limit cycle (Flc_1), which implies that the oscillation patterns of the system become more complex, transitioning to bursting (corresponding to Figs. 2d and f) and chaotic (corresponding to Figs. 2c and e) oscillations. Subsequently, the unstable limit cycle becomes a small stable limit cycle (green curve) through another fold bifurcation of limit cycles (Flc_2), which implies that the oscillation patterns become periodic spiking with small amplitude (corresponding to Fig. 2g). Finally, the small stable limit cycle collides with the unstable equilibrium points at the Hopf bifurcation point (HB) and disappears, resulting in stable equilibrium points (black solid curve), which means the system's behavior becomes quiescent states (corresponding to Fig. 2h).

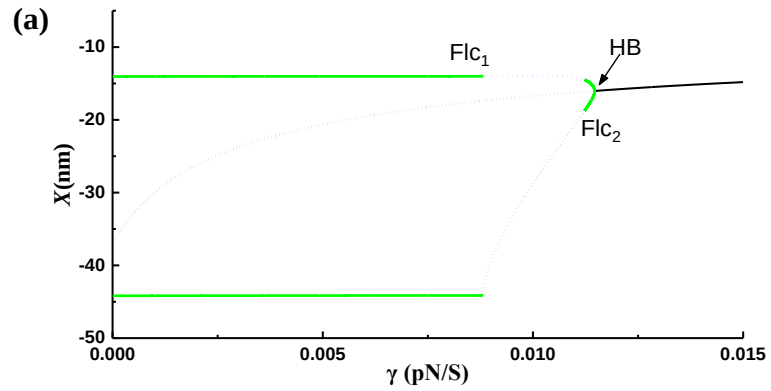

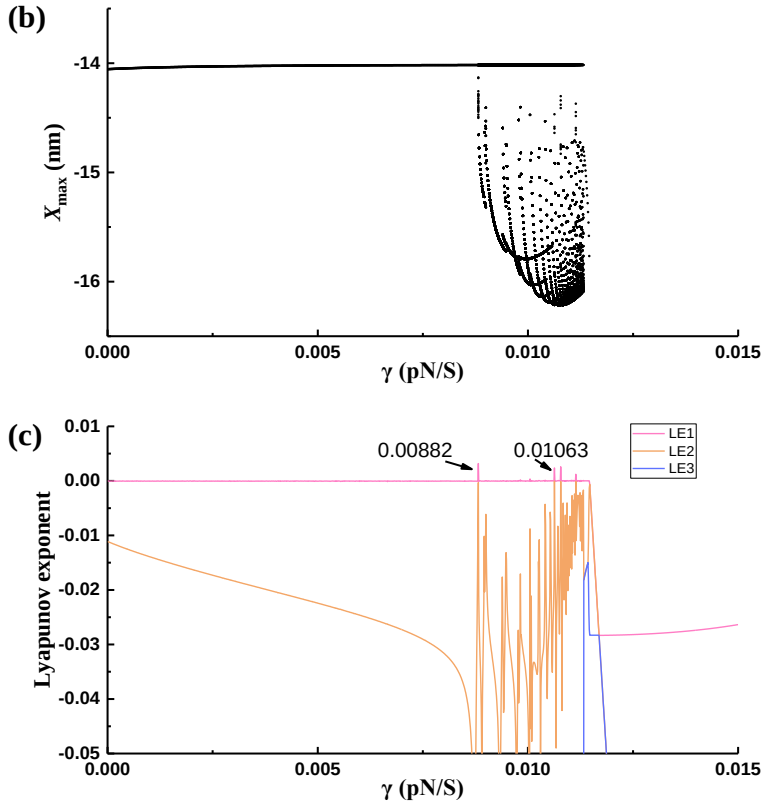

Fig. 3 Bifurcation and chaos analysis of oscillations of hair bundles with respect to γ, for S = 0.95 and D = 70 nm. (a) Equilibrium points and limit cycle bifurcations; (b) Bifurcation diagram of X_{max}; (c) Lyapunov exponent

In addition, the bifurcation of the maximum oscillation values (X_{max}) with γ further validates the transition dynamics of the oscillation patterns from another perspective, as shown in Fig. 3b. When γ is small, the oscillations exhibit a unique maximum value, indicating that the system displays periodic spiking oscillations. As γ increases, multiple X_{max} values appear, indicating that the system transitions to bursting and chaotic oscillations. Subsequently, the system exhibits a single, smaller X_{max} value, indicating a transition to small-amplitude spiking oscillations. Finally, the disappearance of X_{max} signifies that the system has transitioned to a quiescent state. The variation of X_{max} with γ is consistent with the bifurcation analysis and the changes in trajectories with γ. Moreover, the variation of the Lyapunov exponents with γ also supports the previously obtained transition dynamics, as shown in Fig.3c. The values of the maximum Lyapunov exponents (LE1) characterize the patterns of oscillation. When LE1 = 0, the system exhibits periodic oscillations. When LE1 > 0, the system exhibits chaotic oscillations. When LE1 < 0, the system exhibits quiescent state. That is, when the hair bundle exhibits oscillations, it displays periodic oscillations except for a few parameter intervals (such as near γ = 0.00882 and 0.01063) where chaos occurs.

3.3 The impact of memristors on the intervals of oscillation parameters

To further elucidate the impact of memristors on the mechanical oscillation behavior of hair bundles, this section explores how γ affects the parameter intervals of oscillation in the (S, D) parameter plane, with S and D being parameters of particular important in previous studies[13,14].

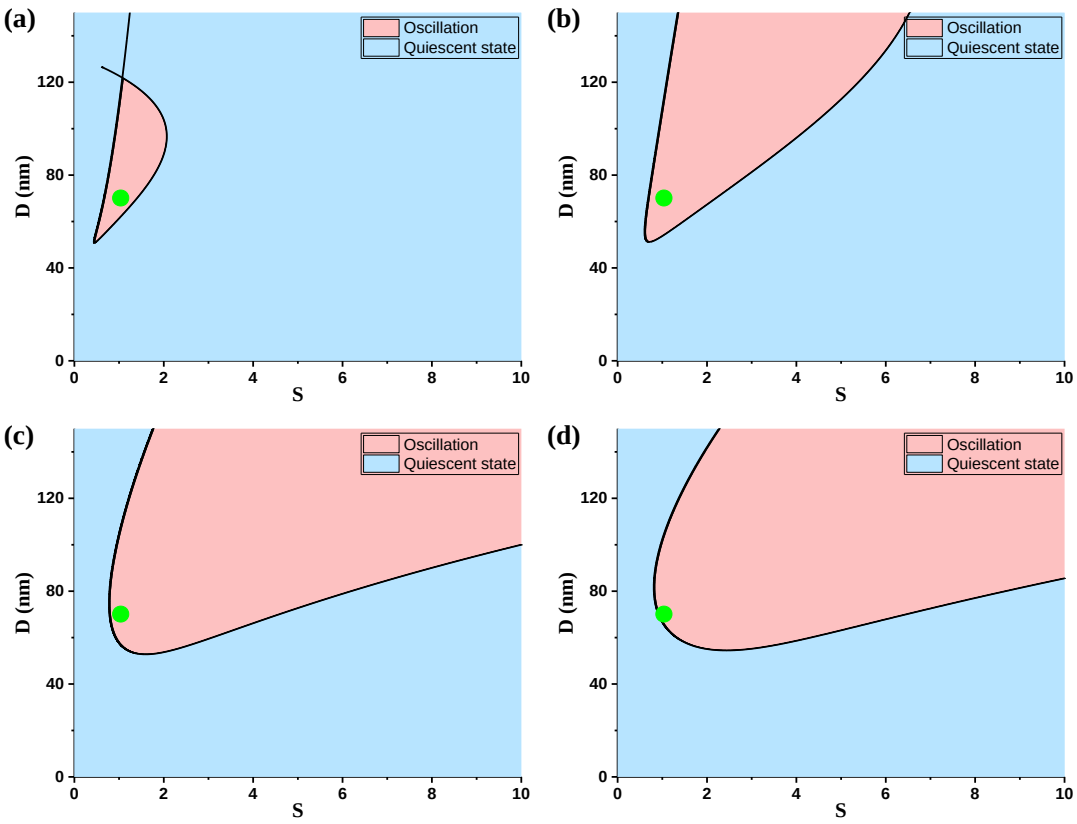

Fig. 4 The impact of γ on the oscillation regions in the (*S*, *D*) two-parameter plane. The black solid curve represents the codimension-2 curve of the Hopf bifurcations. (a) γ = 0 pN/S; (b) γ = 0.001 pN/S; (c) γ = 0.005 pN/S; (d) γ = 0.01 pN/S

In (*D*, *S*) parameter plane, the codimension-2 Hopf bifurcation curve (black solid curve) delineates the boundary between oscillations (red region) and quiescent states (blue region), as shown in Fig. 4. As γ increases, the oscillation region gradually expands towards the upper right, indicating that for larger ranges of *S* and *D*, the action of the memristor with suitable strength can enhance the oscillations of the hair bundle. For smaller values of *S* and *D* (green point, for example, $S = 0.95$, $D = 70$ nm, corresponding to Figs. 2 and 3), as γ increases, the system gradually approaches the edge of the Hopf bifurcation, meaning the system will progressively transition to a quiescent state. An excessively strong memristor action can suppress the oscillations of the hair bundle.

In addition, the codimension-2 Hopf bifurcation curves for different values of γ from Fig. 4 are plotted together in Fig. 5, and the colors, ranging from light to dark, represent the increase in γ. This more clearly illustrates the expansion of the oscillation region and its upward and rightward shift as γ increases. Interestingly, these codimension-2 curves are tangent near $S = 0.86$, $D = 93$ nm (indicated by the arrow), implying that at this parameter value, the memristor has no effect on the oscillations. This parameter insensitivity may reflect the stability of the auditory system under specific physiological conditions, ensuring that external electromagnetic interferences (such as noise or device interventions) do not affect the normal oscillations of the hair bundle, thereby maintaining the reliability of auditory perception.

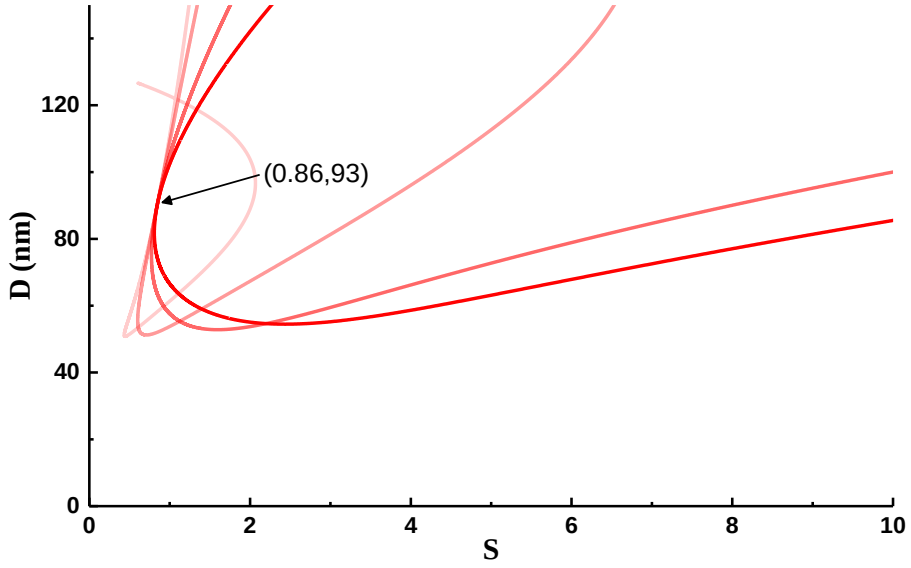

Fig. 5 The distribution of the codimension-2 curve of Hopf bifurcations for γ = 0, 0.001, 0.005 and 0.01 pN/S

4 Conclusion

The hair bundle, as a receiver of sound signals, has mechanical oscillation modes that are crucial for auditory function, and memristors are highly promising components for neuromodulation. This study, for the first time, introduces memristors into the regulation of hair bundle mechanical oscillations. By constructing a dynamical model of hair bundles of auditory hair cell regulated by memristor, it reveals the dynamic regulatory effects of memristor coupling strength (γ) on oscillation patterns. As γ increases, the system successively exhibits periodic spiking, chaotic, bursting, another form of chaos, another form of bursting, and small-amplitude periodic oscillations, eventually entering quiescent state when $\gamma \geq 0.0116$ pN/S. Bifurcation and chaos analyses elucidate the transition dynamics of the oscillation patterns. Bifurcation analysis in the two-parameter plane (S, D) indicates that the rightward shift of the Hopf bifurcation curve suggests that increasing γ can expand the oscillation range of the hair bundle. However, an excessively strong γ can suppress the oscillations, revealing the threshold dependence of memristor regulation. Moreover, the codimension-2 curve of the Hopf bifurcation is tangent at the specific parameter combination (S = 0.86, D = 93 nm), implying that the electromagnetic regulation by the memristor is ineffective at this particular parameter set, and the hair bundle oscillations are insensitive to changes in γ. This finding highlights the robustness and critical characteristics of auditory hair bundle dynamics under specific parameter combinations. It must be clarified that in the model constructed in this paper, the influence of memristors on hair bundles has been somewhat simplified. Further biological experiments and model refinements are needed for validation, which are researched for future research.

In summary, this study elucidates the mechanism of memristor-regulated auditory hair bundle oscillations from a dynamical perspective, providing the possibility for understanding the nonlinear characteristics of auditory function and developing novel neuromodulation technologies.

Reference

[1] Hudspeth A J. Making an effort to listen: mechanical amplification in the ear[J]. Neuron, 2008, 59(4): 530-545.

[2] Hudspeth A J. Integrating the active process of hair cells with cochlear function[J]. Nature Reviews Neuroscience, 2014, 15(9): 600-614.
[3] Hudspeth A J, Martin P. Evolving critical oscillators for hearing[J]. Nature Reviews Physics, 2024, 6(4): 210-211.
[4] Szalai R, Tsaneva-Atanasova K, Homer M E, et al. Nonlinear models of development, amplification and compression in the mammalian cochlea[J]. Philosophical Transactions of the Royal Society A: Mathematical, Physical and Engineering Sciences, 2011, 369(1954): 4183-4204.
[5] Fredrickson-Hemsing L, Strimbu C E, Roongthumskul Y, et al. Dynamics of freely oscillating and coupled hair cell bundles under mechanical deflection[J]. Biophysical Journal, 2012, 102(8): 1785-1792.
[6] Ó Maoiléidigh D, Nicola E M, Hudspeth A J. The diverse effects of mechanical loading on active hair bundles[J]. Proceedings of the National Academy of Sciences of the United States of America, 2012, 109(6): 1943-1948.
[7] Roongthumskul Y, Fredrickson-Hemsing L, Kao A, et al. Multiple-timescale dynamics underlying spontaneous oscillations of saccular hair bundles[J]. Biophysical Journal, 2011, 101(3): 603-610.
[8] Benser M E, Marquis R E, Hudspeth A J. Rapid, active hair bundle movements in hair cells from the bullfrog's sacculus[J]. Journal of Neuroscience, 1996, 16(18): 5629-5643.
[9] Tinevez J Y, Jülicher F, Martin P. Unifying the various incarnations of active hair-bundle motility by the vertebrate hair cell[J]. Biophysical Journal, 2007, 93(11): 4053-4067.
[10] Lin C H J, Bozovic D. Effects of efferent activity on hair bundle mechanics[J]. Journal of Neuroscience, 2020, 40(12): 2390-2402.
[11] Lin C H J, Bozovic D. Efferent activity controls hair cell response to mechanical overstimulation[J]. eNeuro, 2022, 9(4).
[12] Cao B, Gu H, Bai J, et al. Bifurcation and chaos of spontaneous oscillations of hair bundles in auditory hair cells[J]. International Journal of Bifurcation and Chaos, 2021, 31(4): 2130011.
[13] Cao B, Gu H, Ma K. Complex dynamics of hair bundle of auditory nervous system (I): spontaneous oscillations and two cases of steady states[J]. Cognitive Neurodynamics, 2022, 16(4): 917-940.
[14] Cao B, Gu H, Wang R. Complex dynamics of hair bundle of auditory nervous system (II): forced oscillations related to two cases of steady state[J]. Cognitive Neurodynamics, 2021, 3(5): 1163-1188.
[15] Khan W U, Shen Z, Mugo S M, et al. Implantable hydrogels as pioneering materials for next-generation brain–computer interfaces[J]. Chem Soc Rev, 2025.
[16] Xie Y, Ma J. How to discern external acoustic waves in a piezoelectric neuron under noise?[J]. Journal of Biological Physics, 2022, 48(3): 339-353.
[17] Chua L O. Memristor—the missing circuit element[J]. IEEE Transactions on Circuit Theory, 1971, 18(5).
[18] Shao Y, Wu F, Wang Q. Synchronization and complex dynamics in locally active threshold memristive neurons with chemical synapses[J]. Nonlinear Dynamics, 2024, 112(15): 13483-13502.
[19] Wu F, Gu H, Jia Y. Bifurcations underlying different excitability transitions modulated by excitatory and inhibitory memristor and chemical autapses[J]. Chaos, Solitons and Fractals, 2021, 153: 111611.
[20] Wu F, Gu H. Bifurcations of negative responses to positive feedback current mediated by memristor in a neuron model with bursting patterns[J]. International Journal of Bifurcation and Chaos, 2020, 30(4): 1-22.
[21] Wu F, Gu H, Li Y. Inhibitory electromagnetic induction current induces enhancement instead of reduction of neural bursting activities[J]. Communications in Nonlinear Science and Numerical Simulation, 2019, 79: 104924.
[22] Amin Fida A, Khanday F A, Mittal S. An active memristor based rate-coded spiking neural network[J]. Neurocomputing, 2023, 533: 61-71.
[23] Zhou W, Jin P, Dong Y, et al. Memristor neurons and their coupling networks based on Edge of Chaos Kernel[J]. Chaos, Solitons and Fractals, 2023, 177: 114224.
[24] Bao B, Hu J, Bao H, et al. Memristor-coupled dual-neuron mapping model: initials-induced coexisting firing patterns and synchronization activities[J]. Cognitive Neurodynamics, 2024, 18(2): 539–555.
[25] Ying J, Min F, Wang G. Neuromorphic behaviors of VO2 memristor-based neurons[J]. Chaos, Solitons and Fractals, 2023, 175: 114058.

[26] Roongthumskul Y, Faber J, Bozovic D. Dynamics of mechanically coupled hair-cell bundles of the inner ear[J]. Biophysical Journal, 2021, 120(2): 205-216.
[27] Martin P, Hudspeth A J. Compressive nonlinearity in the hair bundle's active response to mechanical stimulation[J]. Proceedings of the National Academy of Sciences of the United States of America, 2001, 98(25): 14386-14391.
[28] Kim K J, Ahn K H. Amplitude death of coupled hair bundles with stochastic channel noise[J]. Physical Review E - Statistical, Nonlinear, and Soft Matter Physics, 2014, 89(4): 1-7.
[29] Yu X, Bao H, Xu Q, et al. Deep brain stimulation and lag synchronization in a memristive two-neuron network[J]. Neural Networks, 2024, 180: 106728.
[30] Zhang X, Li C, Iu H H C, et al. A chaotic memristive Hindmarsh-Rose neuron with hybrid offset boosting[J]. Chaos, Solitons and Fractals, 2024, 185: 115150.
[31] Bard E. Simulating, analyzing, and animating dynamical systems: a guide to XPPAUT for researchers and students[M]. Philadelphia: SIAM, 2002.

[1] **第 1 作者简介:** 曹奔（1997-），男，工学博士，南京信息工程大学，研究方向：神经动力学；分岔与混沌。 E-mail: caoben@nuist.edu.cn。

*** 通讯作者简介:** 曹奔（1997-），男，工学博士，南京信息工程大学，研究方向：神经动力学；分岔与混沌。 E-mail: caoben@nuist.edu.cn。